

REPORT DOCUMENTATION PAGE				Form Approved OMB No. 0704-0188	
Public reporting burden for this collection of information is estimated to average 1 hour per response, including the time for reviewing instructions, searching existing data sources, gathering and maintaining the data needed, and completing and reviewing this collection of information. Send comments regarding this burden estimate or any other aspect of this collection of information, including suggestions for reducing this burden to Department of Defense, Washington Headquarters Services, Directorate for Information Operations and Reports (0704-0188), 1215 Jefferson Davis Highway, Suite 1204, Arlington, VA 22202-4302. Respondents should be aware that notwithstanding any other provision of law, no person shall be subject to any penalty for failing to comply with a collection of information if it does not display a currently valid OMB control number. <b>PLEASE DO NOT RETURN YOUR FORM TO THE ABOVE ADDRESS.</b>					
1. REPORT DATE (DD-MM-YYYY) 03-21-2016		2. REPORT TYPE Interim		3. DATES COVERED (From - To) 15 Jun 2015 – 1 Dec 2015	
4. TITLE AND SUBTITLE nsPEF-induced PIP <sub>2</sub> Depletion, PLC Activity and Actin Cytoskeletal Cortex Remodeling Are Responsible for Post-exposure Cellular Swelling and Blebbing				5a. CONTRACT NUMBER FA8650-13-D-6368-0006	
				5b. GRANT NUMBER N/A	
				5c. PROGRAM ELEMENT NUMBER 62202F	
6. AUTHOR(S)  Gleb P. Tolstykh, Gary L. Thompson, Hope T. Beier, Zachary A. Steelman, and Bennett L. Ibey				5d. PROJECT NUMBER N/A	
				5e. TASK NUMBER N/A	
				5f. WORK UNIT NUMBER HOEB	
7. PERFORMING ORGANIZATION NAME(S) AND ADDRESS(ES)  General Dynamics Information Technology 4141 Petroleum Road JBSA Fort Sam Houston, Texas 78234-2644				8. PERFORMING ORGANIZATION REPORT NUMBER  N/A	
9. SPONSORING / MONITORING AGENCY NAME(S) AND ADDRESS(ES) Air Force Materiel Command Air Force Research Laboratory 711 Human Performance Wing Airman Systems Directorate Bioeffects Division Radio Frequency Bioeffects Branch JBSA Fort Sam Houston, Texas 78234-2644				10. SPONSOR/MONITOR'S ACRONYM(S) 711 HPW/RHDR	
				11. SPONSOR/MONITOR'S REPORT NUMBER(S) AFRL-RH-FS-JA-2016-0009	
12. DISTRIBUTION / AVAILABILITY STATEMENT  Distribution A: Approved for public release; distribution unlimited (P.A. Case No. TSRL-PA-2016-0249, 10 Jun 16).					
13. SUPPLEMENTARY NOTES					
14. ABSTRACT Cell swelling and blebbing has been commonly observed following nanosecond pulsed electric field (nsPEF) exposure. The hypothesized origin of these effects is nanoporation of the plasma membrane (PM) followed by transmembrane diffusion of extracellular fluid and disassembly of cortical actin structures. This investigation will provide evidence that shows passive movement of fluid into the cell through nanopores and increase of intracellular osmotic pressure are not solely responsible for this observed phenomena. We demonstrate that phosphatidylinositol-4,5-bisphosphate (PIP <sub>2</sub> ) depletion and hydrolysis are critical steps in the chain reaction leading to cellular blebbing and swelling. PIP <sub>2</sub> is heavily involved in osmoregulation by modulation of ion channels and also serves as an intracellular membrane anchor to cortical actin and phospholipase C (PLC). Given the rather critical role that PIP <sub>2</sub> depletion appears to play in the response of cells to nsPEF exposure, it remains unclear how its downstream effects and, specifically, ion channel regulation may contribute to cellular swelling, blebbing, and unknown mechanisms of the lasting "permeabilization" of the PM.					
15. SUBJECT TERMS Nanosecond Pulsed Electric Field, nanopores, PIP <sub>2</sub> hydrolysis, cellular swelling and blebbing, calcium					
16. SECURITY CLASSIFICATION OF:			17. LIMITATION OF ABSTRACT	18. NUMBER OF PAGES	19a. NAME OF RESPONSIBLE PERSON
a. REPORT	b. ABSTRACT	c. THIS PAGE			L. Johnson
U	U	U	SAR	6	19b. TELEPHONE NUMBER (include area code) NA



# nsPEF-induced PIP<sub>2</sub> depletion, PLC activity and actin cytoskeletal cortex remodeling are responsible for post-exposure cellular swelling and blebbing

Gleb P. Tolstykh<sup>a,\*</sup>, Gary L. Thompson<sup>b</sup>, Hope T. Beier<sup>c</sup>, Zachary A. Steelman<sup>d</sup>, Bennett L. Ibey<sup>e</sup>

<sup>a</sup> General Dynamics Information Technology, JBSA Fort Sam Houston, TX, USA

<sup>b</sup> Oak Ridge Institute for Science & Education, JBSA Fort Sam Houston, TX, USA

<sup>c</sup> Air Force Research Laboratory, 711th Human Performance Wing, Airman Systems Directorate, Bioeffects Division, Optical Radiation Bioeffects Branch, JBSA Fort Sam Houston, TX, USA

<sup>d</sup> Duke University, Durham, NC, USA

<sup>e</sup> Air Force Research Laboratory, 711th Human Performance Wing, Airman Systems Directorate, Bioeffects Division, Radio Frequency Bioeffects Branch, JBSA Fort Sam Houston, TX, USA

## ARTICLE INFO

### Keywords:

Nanosecond pulsed electric field

Nanopores

PIP<sub>2</sub> hydrolysis

Cellular swelling and blebbing

Calcium

## ABSTRACT

Cell swelling and blebbing has been commonly observed following nanosecond pulsed electric field (nsPEF) exposure. The hypothesized origin of these effects is nanoporation of the plasma membrane (PM) followed by transmembrane diffusion of extracellular fluid and disassembly of cortical actin structures. This investigation will provide evidence that shows passive movement of fluid into the cell through nanopores and increase of intracellular osmotic pressure are not solely responsible for this observed phenomena. We demonstrate that phosphatidylinositol-4,5-bisphosphate (PIP<sub>2</sub>) depletion and hydrolysis are critical steps in the chain reaction leading to cellular blebbing and swelling. PIP<sub>2</sub> is heavily involved in osmoregulation by modulation of ion channels and also serves as an intracellular membrane anchor to cortical actin and phospholipase C (PLC). Given the rather critical role that PIP<sub>2</sub> depletion appears to play in the response of cells to nsPEF exposure, it remains unclear how its downstream effects and, specifically, ion channel regulation may contribute to cellular swelling, blebbing, and unknown mechanisms of the lasting “permeabilization” of the PM.

## 1. Introduction

Exposure to nanosecond pulsed electrical fields (nsPEF) results in a myriad of observable cellular effects, including alteration of intracellular Ca<sup>2+</sup> homeostasis, nuclear granulation, cytoskeletal changes, cellular blebbing, swelling, and initiation of apoptotic cell death [1–8]. While these effects are often attributed to the direct nanoporation of both the plasma and organelle membranes [9–11], the underlying mechanisms are not well understood.

Some of these nsPEF-induced biological effects appear to be similar to situations observed during the normal lifespan of mammalian cells. For example, plasma membrane (PM) blebs occur during cytokinesis, cell migration, proliferation, and apoptosis [12]. It has been shown that both PIP<sub>2</sub> and phosphoinositide-specific PLC are required for regulation of cortical actin dynamics during cytokinesis, since PIP<sub>2</sub> needs to be continuously hydrolyzed for successful completion of cell division, and its hydrolysis pair diacylglycerol (DAG) with protein kinase C (PKC) to stimulate cellular growth and proliferation [13,14]. Likewise, PIP<sub>2</sub> and phosphoinositide-specific PLC are heavily involved in regula-

tion of vital cellular functions such as modulation of PM transport proteins, cytoskeleton dynamics, intracellular Ca<sup>2+</sup> homeostasis, and regulation of cellular volume [15–21]. While alterations of these functions have all been observed after nsPEF exposures, their relation to the nsPEF-induced PIP<sub>2</sub> signaling pathway is not understood.

Recently, we confirmed that a single 16.2 kV/cm, 600 ns electric pulse initiates an intracellular phosphoinositide PIP<sub>2</sub> signaling cascade similar to one initiated by activation of G<sub>q/11</sub>-coupled receptors, but in cells without such receptors [22]. PIP<sub>2</sub> depletion by nsPEF exposure was demonstrated by direct monitoring of translocation of optical probes of PIP<sub>2</sub> hydrolysis. The nsPEF-induced PIP<sub>2</sub> signaling mirrored the responses following human muscarinic acetylcholine G<sub>q/11</sub>-coupled receptor (hM<sub>1</sub>) activation [22,23]. Additionally, the nsPEF-induced increase in intracellular Ca<sup>2+</sup> is almost identical to the calcium rise observed after purinergic P<sub>2</sub>Y<sub>6</sub> G<sub>q/11</sub>-coupled receptor stimulation [24], further suggesting PLC activation and induction of PIP<sub>2</sub> signaling. Initiation of PIP<sub>2</sub> signaling results in production of DAG and inositol-1,4,5-trisphosphate (IP<sub>3</sub>) [25], leading to elevation of cytosolic Ca<sup>2+</sup> from IP<sub>3</sub>-sensitive Ca<sup>2+</sup> stores and DAG – dependent activation of PKC

\* Correspondence to: General Dynamics Information Technology, 4141 Petroleum Road, JBSA Fort Sam Houston, TX 78234, USA.

E-mail address: [gtolstykh@gmail.com](mailto:gtolstykh@gmail.com) (G.P. Tolstykh).

[26].

Permeabilization of the PM by nsPEF is an important step in initiation of the response, but cannot be solely accounted for the long-lasting effects due to the theoretically predicted short lifespan (~100 ns) of nanopores in biomembranes [27]. Cell swelling and blebbing occurs seconds after nsPEF exposure and lasts for minutes, comparable to the time needed for PIP<sub>2</sub> recovery back to the PM [22,23]. Since PIP<sub>2</sub> is known to anchor cortical actin [28] and PLC-dependent PIP<sub>2</sub> hydrolysis modulates cytoplasmic cell volume regulatory ion channels [29,30], we hypothesize that nsPEF-stimulated PLC activity and resulting PIP<sub>2</sub> depletion are primarily responsible for the post-exposure, physiological effects of actin cortex remodeling, cellular swelling, and blebbing. This work aims to further expand our previous findings that disintegration of the cortical actin structures is related to cellular swelling initiated by transmembrane diffusion of water after nsPEF-induced PM nanoporation [7].

## 2. Methods

### 2.1. Nanosecond pulse exposure

Single and multiple (20 at 5 Hz rate) nsPEFs were delivered to cells using a pair of 125 µm-diameter tungsten electrodes spaced 120 µm apart as detailed in previous publications [1,4,22,23]. Finite difference time domain (FDTD) modeling was used to model the exposure system, and FDTD modeling predicted a 16.2 kV/cm peak field for a 1 kV charging voltage (0.5 kV nsPEF amplitude). To synchronize image acquisition and pulse delivery, a Stanford DG535 digital delay generator was programmed to trigger the Zeiss LSM-710 confocal microscope to begin image acquisition. After a 5-s preset delay, a HP 8112 A pulse generator delivered a specific number of nsPEFs.

### 2.2. Probe of PIP<sub>2</sub> hydrolysis

PLC8-PH-EGFP DNA construct (Addgene plasmid 21179) [22,23] was transiently transfected into the Chinese hamster ovarian (CHO) cells already stably expressing m-Apple-actin or G<sub>q11</sub>-coupled hM<sub>1</sub> and angiotensin II (AngII) receptors using a Lonza 2D Nucleofector™ device. Dr. Mark S. Shapiro (Department of Physiology, University of Texas Health Science Center at San Antonio) kindly provided the hM<sub>1</sub> and AngII cells lines [31], and the m-Apple-actin cell line was created in-house as previously described [7].

### 2.3. Experimental procedures

The m-Apple-actin, hM<sub>1</sub>, and AngII receptor stable cell cultures used a standard complete growth medium consisting of Ham's F-12K media supplemented with 10% fetal bovine serum (FBS), 1% penicillin/streptomycin antibiotic, and 0.48% G418 to ensure transfection stability. Cells were plated on poly-L-lysine coated 35 mm glass coverslip bottom dishes (MatTek No. 0, Ashland, MA) for 24 h prior to experimentation. Cells were rinsed to remove any residual growth medium, and 2 mL of a standard buffer solution (pH 7.4, 290–310 mOsm) that consisted of 2 mM MgCl<sub>2</sub>, 5 mM KCL, 10 mM HEPES, 10 mM Glucose, 2 mM CaCl<sub>2</sub>, and 135 mM NaCl was added. In some experiments, the CaCl<sub>2</sub> was replaced with 2 mM K-EGTA to create Ca<sup>2+</sup>-free external buffer.

For intracellular Ca<sup>2+</sup> measurement, CHO-hM<sub>1</sub> cells were loaded with Calcium Green-1 AM ester (CaGr). A 2 µL aliquot of 3 mM CaGr stock was added to 2 mL of standard buffer, and administered to cells incubated at 37 °C for 30 min. After 30 min, the loading buffer was replaced with standard buffer and images were collected using an inverted Zeiss 710 LSM confocal microscope equipped with a 40X (1.3 N.A.) oil immersion objective.

To compare nsPEF effects with well-known effects caused by endogenous PLC activation, some experiments were paired with G<sub>q</sub>/

11-coupled hM<sub>1</sub> receptor agonist oxotremorine (OxoM, 10 µM) or AngII receptor agonist angiotensin II (AngII, 10 µM). In a subset of experiments, cells were incubated with PLC blocker edelfosine (10–20 µM) for 30 min prior to OxoM, AngII, or nsPEF exposure. Agonists were added by circulating fresh bath buffer containing either OxoM or AngII at a flow rate of 2 mL/min. All media, chemicals and pharmaceuticals were obtained from Life Technologies, Tocris Bioscience or Sigma-Aldrich. Also, 4 mM propidium iodide (PI) (BD Bioscience) was added to the external solution during some experiments to verify cell viability.

### 2.4. Data analysis

Cell fluorescence was measured using ImageJ software (NIH) [32]. To measure CaGr fluorescence changes, regions of interest (ROI) were drawn in the cytoplasmic region of cells under study. For PLC8-PH-EGFP and m-Apple-actin fluorescence measurements, ROI were carefully drawn to demark the PM and the cytoplasm of the cell. We used slightly wider ROI during PM measurements to compensate for PM moving during blebbing. Mean fluorescence was measured for each ROI for all images using ImageJ Multi-Measure. Similarly, to measure cell perimeter lengths, ROI were hand-drawn around each cell, and the perimeter was measured. These values were transferred to GraphPad Prism 6 software for statistical analysis and plotting. The responses were calculated for each cell as a percentage difference (ΔF, %) from the mean of the four frames prior to exposure (Baseline) to the frames taken after exposure (Value) using the formula: 100×(Value – Baseline)/Baseline. All imaging experiments were performed at one frame per second (1 Hz).

## 3. Results and discussion

The roles of local cytoskeleton and changes of intracellular hydrostatic pressure in blebbing cells after nsPEF exposure [7] have been studied previously. However, the role that PIP<sub>2</sub> depletion and hydrolysis play in the nsPEF-induced cellular response has not been evaluated. To achieve this goal, we used edelfosine (ET-18-O-CH<sub>3</sub>), a synthetic alkyl-lysophospholipid that blocks PLC to prevent PIP<sub>2</sub> hydrolysis [13,33]. Since edelfosine could arrest cell cycle, inhibit cytokinesis, and initiate apoptosis [13,34–36], we performed a series of experiments to determine its safe operational dose. A small fraction of cells (2%) bathed for 20 min in the 10 µM edelfosine containing buffer experienced PI uptake. However, 100% of the cells had PI uptake after the dose of edelfosine was increased above 30 µM (data not shown). PI uptake is a widely accepted sign of attenuation of cellular viability and PM integrity [37].

To verify the potency of edelfosine as a blocker of PLC activity, we monitored intracellular Ca<sup>2+</sup> release after G<sub>q11</sub>-coupled receptor activation. By using Ca<sup>2+</sup>-chelation in outside buffer, we determined that a 20–30 min pretreatment of cells in 10 µM edelfosine resulted in sufficient decrease of PLC-dependent intracellular Ca<sup>2+</sup> release from the ER (Fig. 1 (A)). In contrast, but similar to our previous observations [23], addition of 10–20 µM edelfosine was unable to completely prevent intracellular Ca<sup>2+</sup> spikes after a single 600 ns, 16.2 kV/cm electric pulse (EP) (Fig. 1 (B)). The persistence of the intracellular Ca<sup>2+</sup> rise suggests that the initial nsPEF-induced PIP<sub>2</sub> depletion is a result of strong, direct mechanical impact on the cellular PM, and not PLC-mediated hydrolysis.

Based on these observations, we chose to use 20 µM of edelfosine to maximally block PLC activity. To outline the critical role of PLC in the cell response to nsPEF, all edelfosine experiments were performed in Ca<sup>2+</sup> containing external buffer. Fig. 2 shows translocation of the PLC8-PH-EGFP construct from the PM to the cytoplasm after G<sub>q11</sub>-coupled receptor stimulation by agonists. This stimulation leads to activation of PLC, which then hydrolyzes PIP<sub>2</sub> to IP<sub>3</sub> and DAG. The PLC8-PH-EGFP construct, with tagged IP<sub>3</sub>, accumulates in the cytoplasm – directly



**Fig. 1.** Edelfosine effect on intracellular phosphoinositide signaling cascade. Edelfosine blocks PLC activity, preventing generation of intracellular IP<sub>3</sub> and intracellular Ca<sup>2+</sup> release. During hM<sub>1</sub> receptor stimulation (A), 10  $\mu\text{M}$  edelfosine prevented intracellular Ca<sup>2+</sup> rises in a time-dependent manner. During nsPEF exposure experiments (B), 10–20  $\mu\text{M}$  edelfosine was unable to prevent a Ca<sup>2+</sup> spike, underlining the initial PLC-independent mechanism. Data are presented as mean of  $\Delta\%$  fluorescence changes with SEM.

demonstrating significant reduction of the PM PIP<sub>2</sub> content (Fig. 2 (A) and (B), after AngII 10  $\mu\text{M}$  and OxoM 10  $\mu\text{M}$  treatment, respectively). This robust PIP<sub>2</sub> hydrolysis process was accompanied by massive cellular blebbing (Fig. 2 (A) and (B) white arrows), providing a link between PIP<sub>2</sub> membrane levels and cell blebbing. Application of 20  $\mu\text{M}$  edelfosine completely blocked the downstream effects of PLC activity, even in the presence of specific G<sub>q/11</sub>-coupled hM<sub>1</sub> receptor agonist OxoM (Fig. 2 (C)). The G<sub>q/11</sub>-dependent PIP<sub>2</sub> hydrolysis caused cellular perimeter changes due to blebbing, but without any PM nanoporation. CHO-AngII cells treated with AngII experienced statistically significant perimeters increase from  $62.3 \pm 1.9 \mu\text{m}$  to  $70.2 \pm 2.4 \mu\text{m}$  (two-tailed *t*-test,  $P=0.014$ ,  $n=23$ ). Similarly the CHO-hM<sub>1</sub> cells treated with OxoM had a perimeter increase from  $41.8 \pm 1.3 \mu\text{m}$  to  $48.07 \pm 1.6 \mu\text{m}$  (two-tailed *t*-test,  $P=0.005$ ,  $n=17$ ). The edelfosine pretreated AngII and hM<sub>1</sub> cells had no blebbing, perimeter decrease, and no significant perimeter increase after agonist application (Fig. 2 (C)).

Similar to G<sub>q/11</sub>-receptors stimulation, single and multiple 16.2 kV/cm nsPEF exposures caused PIP<sub>2</sub> depletion in CHO-hM<sub>1</sub> cells with consequential cell swelling and blebbing. Pretreatment of cells with edelfosine significantly reduced post-exposure cellular perimeter changes and eliminated cell blebbing from a single 16.2 kV/cm pulse. A slight increase of post exposure cellular perimeter was observed after one 16.2 kV/cm EP (from  $41.1 \pm 1.1 \mu\text{m}$  to  $42.4 \pm 1.1 \mu\text{m}$ ,  $P=0.432$ ), and the increase was more noticeable after twenty 16.2 kV/cm EPs

(from  $44.9 \pm 2.29 \mu\text{m}$  to  $48.7 \pm 2.48 \mu\text{m}$ ,  $P=0.296$ ). The summaries of delta percent ( $\Delta\%$ ) changes of cell perimeter are presented in Fig. 2 (D). The  $\Delta\%$  changes were: CHO-hM<sub>1</sub>  $9.8 \pm 3$  ( $n=20$ ); CHO-AngII  $11.5 \pm 2.5$  ( $n=25$ ); and  $5.9 \pm 2.3$  ( $n=15$ ),  $24.2 \pm 2.6$  ( $n=13$ ) for 1 and 20, 600 nsPEFs, respectively. In edelfosine-treated groups  $\Delta\%$  changes were:  $-3.8 \pm 1.4$  for CHO-hM<sub>1</sub> ( $n=12$ );  $-0.77 \pm 0.99$  CHO-AngII ( $n=16$ );  $1.9 \pm 0.6$  and  $6.9 \pm 2.1$  for 1 and 20, 600 nsPEFs ( $n=11$  and 6).

Blebbing after G<sub>q/11</sub>-receptor stimulation or nsPEF exposure appears to share similar core mechanisms, as blocking PLC activity with edelfosine was able to prevent blebbing in both G<sub>q/11</sub>-receptor agonists and a single nsPEF pulse case and decrease its occurrence in multiple pulse experiments. This persistence of some blebbing in nsPEF-exposed cells could be related to nsPEF-induced nanoporation of the PM, which leads to slight perimeter increase due to cell swelling, in addition to alterations of PIP<sub>2</sub>-dependent cell osmoregulation.

A recent study of fixation-induced cell blebbing demonstrated a correlation between blebbing and PIP<sub>2</sub> levels at the PM. In summary, cell fixation-induced blebbing was reduced in PIP<sub>2</sub>-containing cells but occurred in PIP<sub>2</sub>-depleted cells. Moreover, lowering of the PIP<sub>2</sub> level at cytoskeleton-attaching membrane sites caused bleb formation at these sites [38]. As we have shown that the PIP<sub>2</sub>-depletion response appears to persist in nsPEF-exposed cells even after blocking PLC (Fig. 1 (B)), we investigated the relationship between local PIP<sub>2</sub> depletion and cellular blebbing after nsPEF exposure. Surface plots created on cells

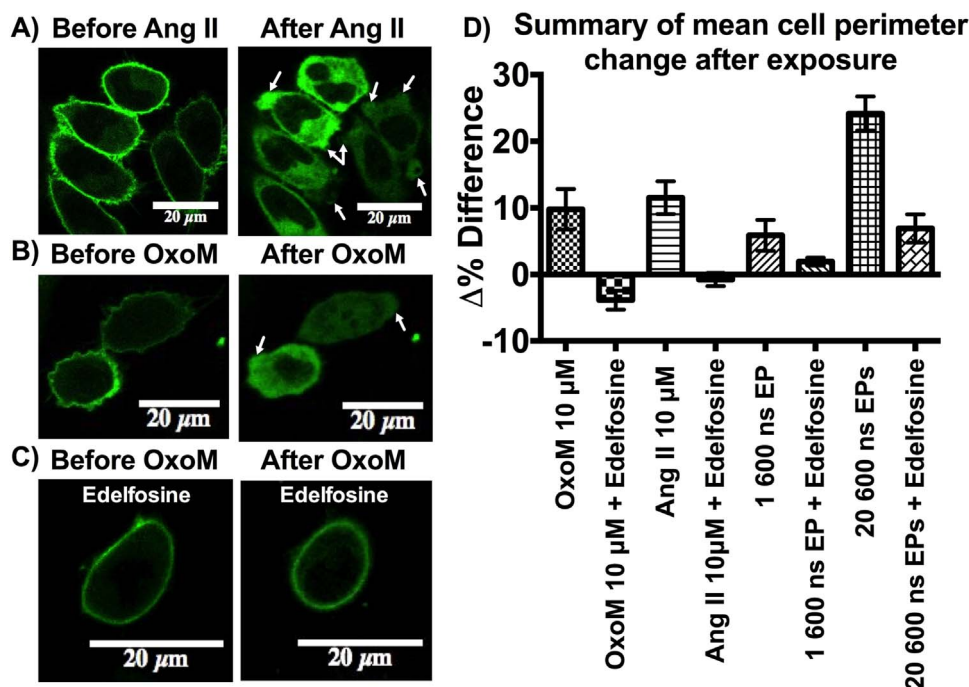


**Fig. 2.** PIP<sub>2</sub> depletion and related post-exposure changes in cell perimeter. Stimulation of G<sub>q/11</sub>-receptors by agonists resulted in PLC8-PH-EGFP probe translocation from membrane to cytoplasm (signifying PIP<sub>2</sub> hydrolysis) and cellular blebbing with a relative increase of cellular perimeter (A and B). As expected, 20  $\mu\text{M}$  edelfosine prevented such translocation but resulted in a decrease of cellular perimeter (C). A summary of cellular perimeter changes is presented on (D). Data are presented as mean of  $\Delta\%$  fluorescence changes with SEM.



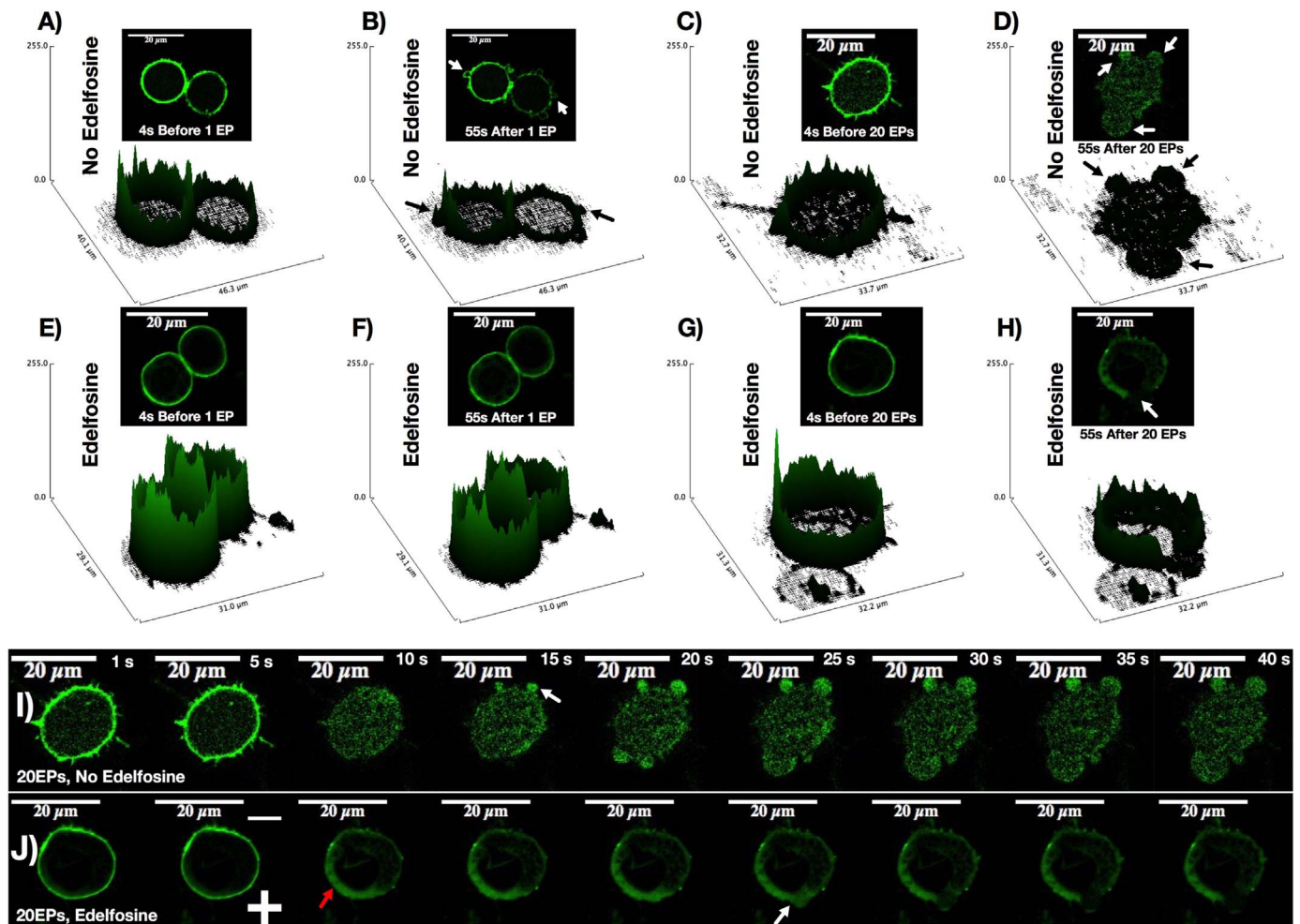


**Fig. 3.** Effect of PLC blockage on nsPEF induced  $\text{PIP}_2$  cellular effects. nsPEF exposures resulted in  $\text{PIP}_2$  depletion, as tracked by PLC6-PH-EGFP probe translocation, and cellular blebbing (A, B, C, D). 20  $\mu\text{M}$  edelfosine pretreatment prevented all these effects after a single, 16.2 kV/cm, 600 ns EP (E and F). Twenty pulses resulted in partial  $\text{PIP}_2$  depletion on the cell side facing the anodic electrode, with single bleb formation in the same location (G and H). Time lapse of post- 20 pulses of 16.2 kV/cm nsPEF exposure shows cellular effects in normal (I) and edelfosine-treated (J) cells.

before and after single or multiple pulsed EF exposures materialize like a fluorescent ring surrounding the cytoplasm due to strong localization of the PLC6-PH-EGFP construct to the PM (Fig. 3 (A-H)). Lowering of  $\text{PIP}_2$  content after nsPEF-induced  $\text{PIP}_2$  depletion resulted in reduction of PM fluorescence due to PLC6-PH-EGFP translocation to the cytoplasm, as demonstrated by disappearance of the fluorescent ring (Fig. 3 (A) vs. (B) for 1, 16.2 kV/cm 600 nsPEF; (C) vs. (D) for 20, 16.2 kV/cm 600 nsPEFs). Post-exposure cellular blebbing occurred at areas of maximum  $\text{PIP}_2$  depletion (Fig. 3 (B) and (D), white and black arrows). Pretreatment of cells with 20  $\mu\text{M}$  edelfosine blocked PLC and prevented  $\text{PIP}_2$  depletion, preserving the fluorescent ring in place after exposure (Fig. 3 (E) vs. (F) for 1, 16.2 kV/cm 600 nsPEF; (G) vs. (H) for 20, 16.2 kV/cm 600 nsPEFs). The post-exposure rate of translocation of PLC6-PH-EGFP from PM to cytoplasm was significantly reduced in edelfosine-treated groups (Fig. 3, (F) vs. (B), and (H) vs. (D)). Note that in the edelfosine-treated group, 20, 16.2 kV/cm 600 nsPEFs caused strong  $\text{PIP}_2$  depletion only in the area of the highest field (anode facing), where the bleb formed (Fig. 3 (H), white and black arrows).

The time-course of the  $\text{PIP}_2$  depletion and cell blebbing from these multiple pulse exposures are demonstrated in Figs. 3 (I) and 3 (J). Complete  $\text{PIP}_2$  depletion was observed after application of 20, 16.2 kV/cm 600 nsPEFs immediately after exposure (Fig. 3 (I), 10 s), and cellular blebbing was observed 10 s after exposure (Fig. 3 (I), 15 s, white arrow). In edelfosine-pretreated cells, a similar exposure to 20

nsEPs produced  $\text{PIP}_2$  depletion only on the cell side facing the anodic electrode (Fig. 3 (J), 10 s, red arrow). This observation suggests direct effect of nsPEF exposure on the PM. The underlying mechanism for such a direct effect on the PM remains elusive with possibilities being a stimulus due to mechanical waves or electrophoretic flow, localized reactive oxygen species, or electrodeformation-induced stretch [39–41].

Blebs were formed with a significant time delay of 20 s after exposure (Fig. 3 (J), white arrow), and bleb formation was related to complete local  $\text{PIP}_2$  depletion. Thus, cell blebbing after nsPEF impact or  $\text{G}_{\text{q11}}$ -receptors stimulation might be directly related to alteration of the  $\text{PIP}_2$  - PM - cortical actin structure. Cortical actin dissociation was linked earlier to blebbing of erythrocytes in patients with chorea-acanthocytosis [42]. In CHO cells, similar observations were reported as a downstream effect of nsPEF exposure [7]. However, the relation between cortical actin disassembly and PM  $\text{PIP}_2$  depletion was not demonstrated. To study this relationship, we transiently transfected stable CHO-m-Apple-actin cells with PLC6-PH-EGFP construct. A 20 16.2 kV/cm 600 nsEPs produced observable  $\text{PIP}_2$  depletion 2 s after exposure (green arrows highlight depletion). Conversely, the m-Apple actin distribution is not affected 2 s post exposure (Fig. 4 (A)). According to our previous experiments [23], the peak of PLC6-PH-EGFP translocation into the cytoplasm occurs within 9 s after exposure. Surprisingly, at 9 s after nsPEF exposure, we noted dimming of the cortical actin fluorescence, and correspondingly, blebbing started in the

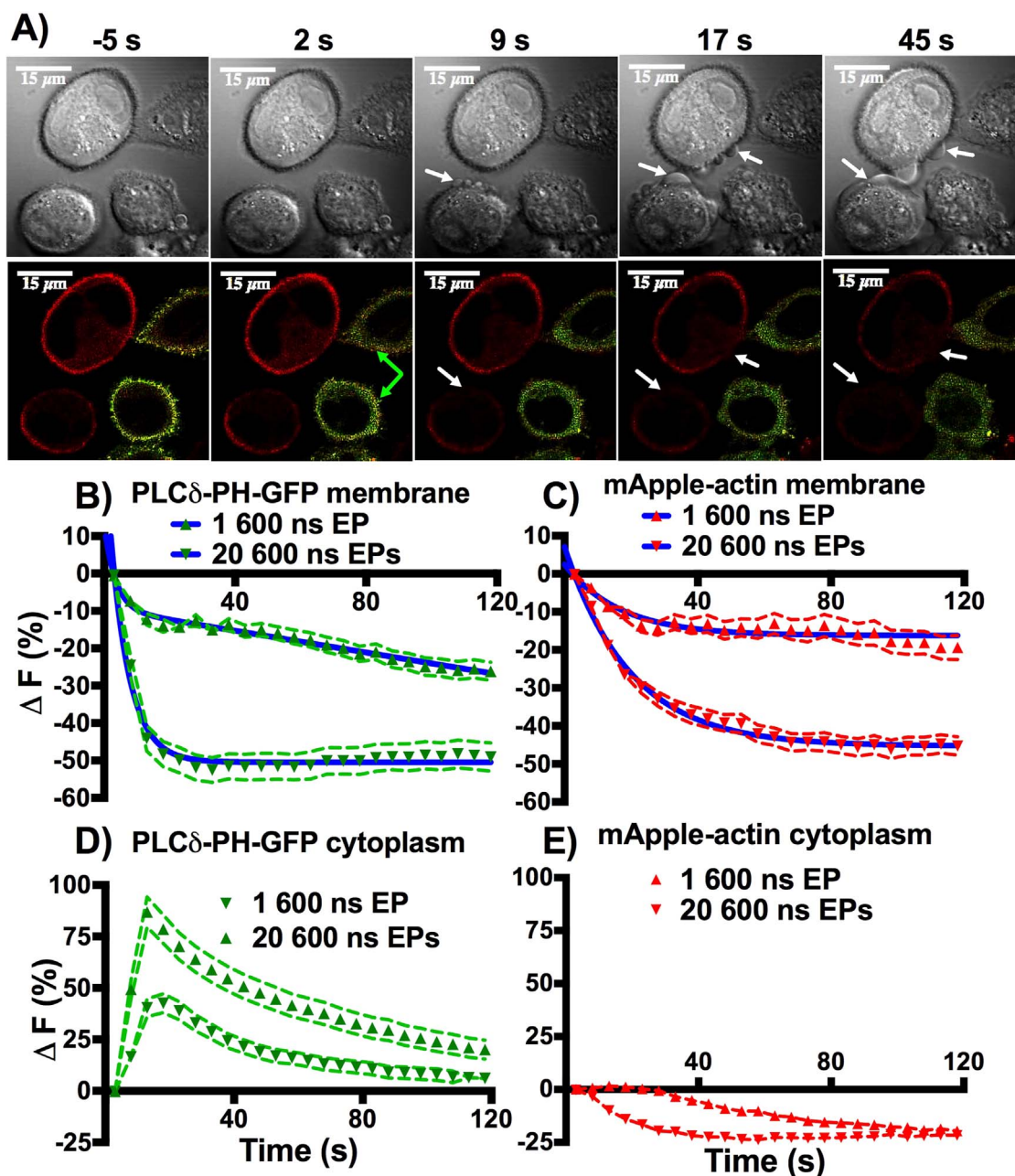


**Fig. 4.** Actin cortex and  $\text{PIP}_2$  changes after nsPEF exposure. Actin cortex dissociation is directly related to  $\text{PIP}_2$  depletion and cellular blebbing (A). Rapid PLC $\delta$ -PH-EGFP probe translocation is observed after nsPEF exposure (B and D). A slower decrease in mApple-actin cortex fluorescence is also observed after nsPEF exposure (C), but without accumulation in the cytoplasm (E). Data are presented as mean of  $\Delta\%$  fluorescence changes with SEM.

same region of the PM (Fig. 4 (A)), at 9 s, white arrows). Thus, actin cortex dissociation follows nsPEF-induced  $\text{PIP}_2$  depletion in an EF dose-dependent manner. After nsPEF exposure, PLC $\delta$ -PH-EGFP transfected cells show a decrease in PM fluorescence and an increase in cytoplasmic fluorescence (Fig. 4 (B) and (D)). Conversely, only a decrease of PM fluorescence was noted in the mApple-actin group (Fig. 4 (C) and (E)), suggesting actin cortex dissociation and not fluorescent crosstalk from the PLC $\delta$ -PH-EGFP emission. Exponential decay analysis revealed a best-fit using two-phase decay ( $\tau_{\text{fast}} \sim 6$  s for 20 P and  $\sim 4$  s for 1 P) for PLC $\delta$ -PH-EGFP response and one phase decay for m-Apple-actin response ( $\tau \sim 17$  s for 20 P and  $\sim 11$  s for 1 P) (Fig. 4 (B) and (C), blue lines). This finding confirms that actin cortex dissociation follows  $\text{PIP}_2$  depletion temporally.

Despite the myriad of reported cell effects after nsPEF (both acute and long term) exposure, we believe that these observations share a

root physiological mechanism, namely  $\text{PIP}_2$  depletion and PLC activation. This activation is strikingly similar to that observed during  $\text{G}_{q11}$ -receptor mediated responses to pharmaceutical stimuli. In previous papers, we showed that nsPEF can cause depletion of  $\text{PIP}_2$  and activation of PLC in the absence of calcium and that effect appears predominately on the anode portion of the PM [23]. In this paper, we have shown that  $\text{PIP}_2$  depletion, PLC activity, and subsequent actin cortex dissociation are the likely origins of the well-documented cellular swelling and blebbing observed after nsPEF exposure. If we accept that  $\text{PIP}_2$  depletion and downstream consequences of this depletion occur during nsPEF stimulation, then the role of ion channels and intracellular enzymes in the response of cells to nsPEF cannot be ignored. Furthermore, longer-term consequences such as sensitization, stimulation, and cell death are also related directly to  $\text{PIP}_2$  depletion. From this work and previous papers, it is clear that nsPEF-induced

biophysical response is both a physical interaction between the field and the membranes of cells and a resultant biological/biochemical reaction occurring in specific cellular initiated pathways. What remains unclear is the biophysical mechanism(s) underlying nanoporation and depletion of PIP<sub>2</sub> and their further interrelations on the molecular level. Such understanding will be the focus of future work.

## Acknowledgments

This work was supported by the Air Force Office of Scientific Research LRIR #13RH08COR. We would like to thank Dr. Mark S. Shapiro for providing CHO cell lines and Ms. Melissa Tarango for technical assistance during our experiments.

## Appendix A. Transparency document

Supplementary data associated with this article can be found in the online version at <http://dx.doi.org/10.1016/j.bbrep.2016.11.005>.

## References

- [1] C.C. Roth, G.P. Tolstykh, J.A. Payne, et al., Nanosecond pulsed electric field thresholds for nanopore formation in neural cells, *J. Biomed. Opt.* 18 (2013) 035005.
- [2] G.L. Craviso, P. Chatterjee, G. Maalouf, et al., Nanosecond electric pulse-induced increase in intracellular calcium in adrenal chromaffin cells triggers calcium-dependent catecholamine release, *Dielectrics and Electrical Insulation, IEEE Trans. on* 16 (2009) 1294–1301.
- [3] H.T. Beier, C.C. Roth, G.P. Tolstykh, et al., Resolving the spatial kinetics of electric pulse-induced ion release, *Biochem Biophys. Res Commun.* 423 (2012) 863–866.
- [4] G.L. Thompson, C. Roth, G. Tolstykh, et al., Disruption of the actin cortex contributes to susceptibility of mammalian cells to nanosecond pulsed electric fields, *Bioelectromagnetics* 35 (2014) 262–272.
- [5] S.J. Beebe, P.F. Blackmore, J.A. White, et al., Nanosecond pulsed electric fields modulate cell function through intracellular signal transduction mechanisms, *Physiol. Meas.* 25 (2004) 1077–1093.
- [6] S.J. Beebe, P.M. Fox, L.J. Rec, et al., Nanosecond, high-intensity pulsed electric fields induce apoptosis in human cells, *FASEB J.* 17 (2003) 1493–1495.
- [7] A.G. Pakhomov, S. Xiao, O.N. Pakhomova, et al., Disassembly of actin structures by nanosecond pulsed electric field is a downstream effect of cell swelling, *Bioelectrochemistry* 100 (2014) 88–95.
- [8] M.A. Rassokhin, A.G. Pakhomov, Cellular regulation of extension and retraction of pseudopod-like blebs produced by nanosecond pulsed electric field (nsPEF), *Cell Biochem Biophys.* 69 (2014) 555–566.
- [9] A.G. Pakhomov, J.F. Kolb, J.A. White, et al., Long-lasting plasma membrane permeabilization in mammalian cells by nanosecond pulsed electric field (nsPEF), *Bioelectromagnetics* 28 (2007) 655–663.
- [10] O.M. Nesin, O.N. Pakhomova, S. Xiao, et al., Manipulation of cell volume and membrane pore comparison following single cell permeabilization with 60- and 600 ns electric pulses, *Biochim Biophys. Acta* 2011 (1808) 792–801.
- [11] L. Chopinet, M.-P. Rols, Nanosecond electric pulses: a mini-review of the present state of the art, *Bioelectrochemistry* (2014).
- [12] G. Charras, E. Paluch, Blebs lead the way: how to migrate without lamellipodia, *Nat. Rev. Mol. Cell Biol.* (9) (2008) 730–736.
- [13] R. Wong, L. Fabian, A. Forer, et al., Phospholipase C and myosin light chain kinase inhibition define a common step in actin regulation during cytokinesis, *BMC Cell Biol.* 8 (2007) 15.
- [14] M. Serova, A. Ghoul, K.A. Benhadji, et al., Preclinical and clinical development of novel agents that target the protein kinase C family, *Semin Oncol.* 33 (2006) 466–478.
- [15] N. Gamper, Osmosensitivity through the PIP<sub>2</sub> availability: just add water, *J. Physiol.* 588 (2010) 3631–3632.
- [16] N. Gamper, V. Reznikov, Y. Yamada, et al., Phosphatidylinositol 4,5-bisphosphate signals underlie receptor-specific Gq/11-mediated modulation of N-type Ca<sup>2+</sup> channels, *J. Neurosci.* 24 (2004) 10980–10992.
- [17] N. Gamper, M.S. Shapiro, Regulation of ion transport proteins by membrane phosphoinositides, *Nat. Rev. Neurosci.* 8 (2007) 921–934.
- [18] M.J. Berridge, Inositol trisphosphate and calcium signalling mechanisms, *Biochim Biophys. Acta* 2009 (1793) 933–940.
- [19] D. Raucher, T. Stauffer, W. Chen, et al., Phosphatidylinositol 4,5-bisphosphate functions as a second messenger that regulates cytoskeleton-plasma membrane adhesion, *Cell* 100 (2000) 221–228.
- [20] S.G. Rhee, Regulation of phosphoinositide-specific phospholipase C, *Annu Rev. Biochem.* 70 (2001) 281–312.
- [21] S.G. Rhee, Y.S. Bae, Regulation of phosphoinositide-specific phospholipase C isozymes, *J. Biol. Chem.* 272 (1997) 15045–15048.
- [22] G.P. Tolstykh, H.T. Beier, C.C. Roth, et al., Activation of intracellular phosphoinositide signaling after a single 600 ns electric pulse, *Bioelectrochemistry* 94C (2013) 23–29.
- [23] G.P. Tolstykh, H.T. Beier, C.C. Roth, et al., 600ns pulse electric field-induced phosphatidylinositol-bisphosphate depletion, *Bioelectrochemistry* (2014).
- [24] J.A. White, P.F. Blackmore, K.H. Schoenbach, et al., Stimulation of capacitative calcium entry in HL-60 cells by nanosecond pulsed electric fields, *J. Biol. Chem.* 279 (2004) 22964–22972.
- [25] S.B. Lee, S.G. Rhee, Significance of PIP<sub>2</sub> hydrolysis and regulation of phospholipase C isozymes, *Curr. Opin. Cell Biol.* 7 (1995) 183–189.
- [26] E. Oancea, T. Meyer, Protein kinase C as a molecular machine for decoding calcium and diacylglycerol signals, *Cell* 95 (1998) 307–318.
- [27] Z.A. Levine, P.T. Vernier, Life cycle of an electropore: field-dependent and field-independent steps in pore creation and annihilation, *J. Membr. Biol.* 236 (2010) 27–36.
- [28] S.P. Denker, D.L. Barber, Ion transport proteins anchor and regulate the cytoskeleton, *Curr. Opin. Cell Biol.* 14 (2002) 214–220.
- [29] J. Piron, F.S. Choveau, M.Y. Amarouch, et al., KCNE1-KCNQ1 osmoregulation by interaction of phosphatidylinositol-4,5-bisphosphate with Mg<sup>2+</sup> and polyamines, *J. Physiol.* 588 (2010) 3471–3483.
- [30] F. Lang, M. Foller, K. Lang, et al., Cell volume regulatory ion channels in cell proliferation and cell death, *Methods Enzym.* 428 (2007) 209–225.
- [31] N. Gamper, J.D. Stockand, M.S. Shapiro, The use of Chinese hamster ovary (CHO) cells in the study of ion channels, *J. Pharm. Toxicol. Methods* 51 (2005) 177–185.
- [32] W.S. Rasband, ImageJ, <http://rsbweb.nih.gov/ij/>, 2008.
- [33] L.F. Horowitz, W. Hirdes, B.-C. Suh, et al., Phospholipase C in living cells activation, inhibition, Ca<sup>2+</sup> requirement, and Regulation of M current, *J. Gen. Physiol.* 126 (2005) 243–262.
- [34] A. Ausili, A. Torrecillas, F.J. Aranda, et al., Edelfosine is incorporated into rafts and alters their organization, *The journal of physical chemistry, B* 112 (2008) 11643–11654.
- [35] C. Gajate, F. Mollinedo, Edelfosine and perifosine induce selective apoptosis in multiple myeloma by recruitment of death receptors and downstream signaling molecules into lipid rafts, *Blood* 109 (2007) 711–719.
- [36] F. Mollinedo, C. Gajate, S. Martin-Santamaria, et al., ET-18-OCH<sub>3</sub> (edelfosine): a selective antitumour lipid targeting apoptosis through intracellular activation of Fas/CD95 death receptor, *Curr. Med. Chem.* 11 (2004) 3163–3184.
- [37] Y. Yang, Y. Xiang, M. Xu, From red to green: the propidium iodide-permeable membrane of *Shewanella decolorationis* S12 is repairable, *Sci. Rep.* 5 (2015) 18583.
- [38] S. Zhao, H. Liao, M. Ao, et al., Fixation-induced cell blebbing on spread cells inversely correlates with phosphatidylinositol 4,5-bisphosphate level in the plasma membrane, *FEBS Open Bio* 4 (2014) 190–199.
- [39] C.C. Roth, R.A. Barnes, B.L. Ibey, et al., Cells exposed to nanosecond electrical pulses exhibit biomarkers of mechanical stress, 2015, pp. 932612–932612–932618.
- [40] C.C. Roth, S. Maswadi, B.L. Ibey, et al., Characterization of acoustic shockwaves generated by exposure to nanosecond electrical pulses, 2014, pp. 894110–894110–894110.
- [41] O.N. Pakhomova, V.A. Khorokhorina, A.M. Bowman, et al., Oxidative effects of nanosecond pulsed electric field exposure in cells and cell-free media, *Arch. Biochem Biophys.* 527 (2012) 55–64.
- [42] M. Foller, A. Hermann, S. Gu, et al., Chorea-sensitive polymerization of cortical actin and suicidal cell death in chorea-acanthocytosis, *FASEB J.* 26 (2012) 1526–1534.